THE BARYON FRACTION IN FIVE GALAXY GROUPS

N. Martinet[2][1], F. Durret[2], T. F. Laganá[3] and G. B. Lima Neto[3]

Abstract. Using ESO 2.2m/WFI optical data in two bands, we computed the galaxy luminosity functions of five groups of galaxies, selecting group members with the color-magnitude relation. By integrating the luminosity function, we calculated the stellar masses of our groups. We then calculated the X-ray gas mass and the total group mass from the density and temperature profiles obtained from XMM-Newton X-ray data. This enabled us to derive the baryon fraction in our groups and to compare it with those from other studies of groups and clusters.

Keywords: groups of galaxies, optical, X-rays

1   Introduction

Groups of galaxies are composed of a few to a few tens of galaxies in gravitational quasi-equilibrium. As for clusters, their principal baryonic constituents are the stellar matter, mainly inside galaxies and the intracluster gas. The former is detected through optical observations (among other wavelength) and the latter mainly through X-rays.

These data give access to the fraction of baryons inside groups. Similar studies have been conducted on clusters of galaxies (e.g. Laganá et al. 2008, Giodini et al. 2009) and on small clusters (e.g. Vikhlinin et al. 2006, Sun et al. 2009, Andreon 2010). In most cases, only the gas mass is calculated. Then, the stellar mass is considered as one fifth or one sixth of the gas mass, and the baryon fraction is estimated.

This last assertion, true for clusters, is discussed in the case of groups. We confirm here that the stellar matter contributes as much as the gas to the baryon budget in the case of groups. This could be a first step to answering recent questions about the nature of groups. Are they scaled-down clusters or are they more specific objects?

We present here the methods we used to estimate the baryon fractions of five groups of galaxies: NGC4325, HCG62, HCG42, NGC5044 and NGC5846. This work was based on ESO 2.2m/WFI data in the B and Rc optical bands and XMM-*Newton* X-ray data. Our results are put in perspective with other baryon fractions of low mass clusters.

2   Optical analysis

Optical WFI images are treated using SExtractor (Bertin & Arnouts 1996), SCAMP (Bertin 2006) and SWarp (Bertin 2002). Then, R and B magnitudes of objects are extracted via the MAG_AUTO keyword of SExtractor. Magnitudes are corrected for airmass and extinction. This last correction is done with the extinction maps from Schlegel et al. (1998).

The analysis leading to an estimate of the stellar mass is done following statistical methods used for clusters (see e.g. Durret et al. 2009). Galaxies are separated from stars based on their central surface brightness. We checked that the number of stars found per square degree is consistent with the Besançon catalog (Robin et al. 2003). Galaxies belonging to the group are then selected from a (B-R) versus R color magnitude relation based on galaxies with spectroscopic redshifts (Fig. 1, left). One can note that statistical subtraction of galaxy counts

[1] ENS de Cachan, 94230 Cachan, France

[2] UPMC Université Paris 06, UMR 7095, Institut d'Astrophysique de Paris, 98bis Bd Arago, F-75014, Paris, France

[3] IAG, USP, R. do Matão 1226, 05508-090, São Paulo/SP, Brazil
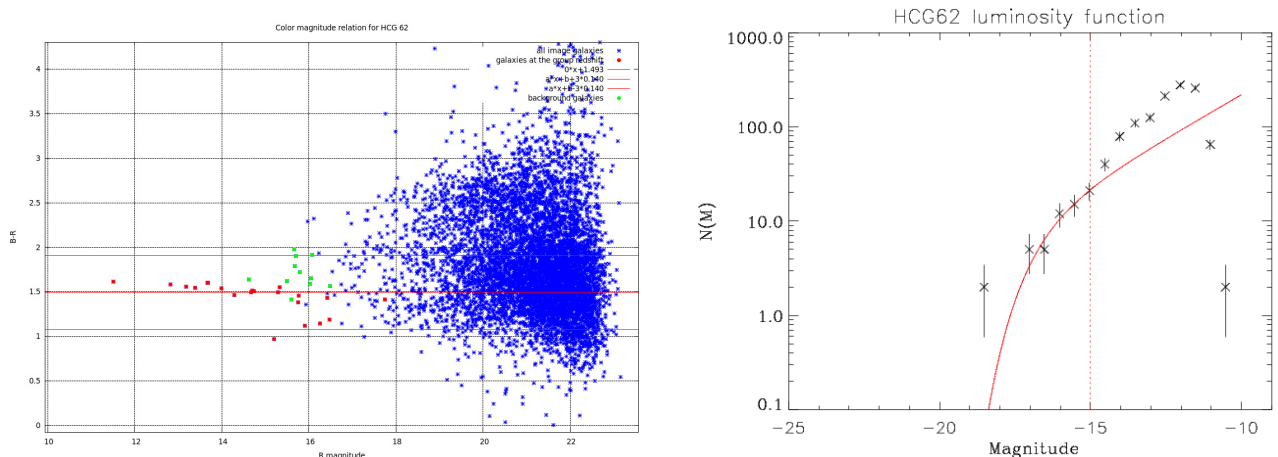
Fig. 1. Left: HCG62 B-R vs. R color magnitude relation. Red dots are the galaxies which belong to the group according to their spectroscopic redshift. Red lines indicate the $\pm 3\sigma$ red sequence. Green dots are background galaxies with a measured spectroscopic redshift. **Right:** HCG62 R-band luminosity function. The red curve is the Schechter fit of the data down to an absolute magnitude of -15 (dotted line)

is not possible in the case of groups due to the small number of galaxies. After selecting the galaxies belonging to the group, we can plot the luminosity function of the groups in their r_{2500} radius (the radius at which the group reaches 2500 times the critical density of the Universe) and fit them with a Schechter function. One can see on the right side of Fig. 1 that the Schechter function is divided in two parts. The bright part corresponds to the bright galaxies and seems to be the Schechter function of the group, while the faint part shows higher counts dominated by background galaxies. An estimate of the mass is obtained by integration of this function. Luminosities are converted into masses using different M/L ratios for elliptical and spiral galaxies. These ratios are taken from Kauffmann et al. (2003) and the fraction of spiral galaxies from Osmond & Ponman (2004).

However, these statistical methods, which are applicable for clusters, are not well suited to groups. This can be seen if we plot the color-magnitude relation for all the galaxies with known redshift. One can see on the left part of Fig. 1 that background galaxies (green dots) are not well separated from galaxies belonging to the group (red dots). In the case of clusters, those background galaxies can be neglected (at least at relatively bright magnitudes) due to their faint number compared to the large amount of cluster galaxies. Taking this into account, a Schechter function cannot correctly fit the data and we finally calculated the mass in a different way, by considering that the stellar mass is the mean of an upper and lower limit. The lower limit is obtained by simply adding the masses of the galaxies belonging to the group according to their spectroscopic redshift. The upper limit is obtained by adding the masses of all the galaxies within the red sequence limits (color magnitude best fit $\pm 3\sigma$). The error bars, given by the differences between the upper and mean values, are considerably below the error bars due to the missknowledge of the mass to luminosity ratios.

3   X-ray analysis

XMM-*Newton* X-ray data were reduced using the standard procedure with the SAS package[*]. The time intervals of high particle background (flares) have been removed and we have produced clean event files for the pn, MOS1 and MOS2. We have used normalized blank-fields[†] to compute the necessary background spectra.

The temperature profiles were determined in concentric circular rings around the centre where, for each ring we have extracted the spectra form all EPIC cameras and produced the appropriated RMF and ARF. For each ring we have fitted the spectra using XSPEC 12, with a plasma emission model MEKAL and photoelectric absorption model PHABS.

The gas density profile was deprojected from the radial surface brightness profiles, which were measured using the task ELLIPSE from IRAF. We have used exposure map corrected [0.5–8.0 keV] images from the MOS

---

[*]See http://xmm.esac.esa.int/sas/current/howtousesas.shtml

[†]See http://xmm2.esac.esa.int/external/xmm_sw_cal/background/index.shtml
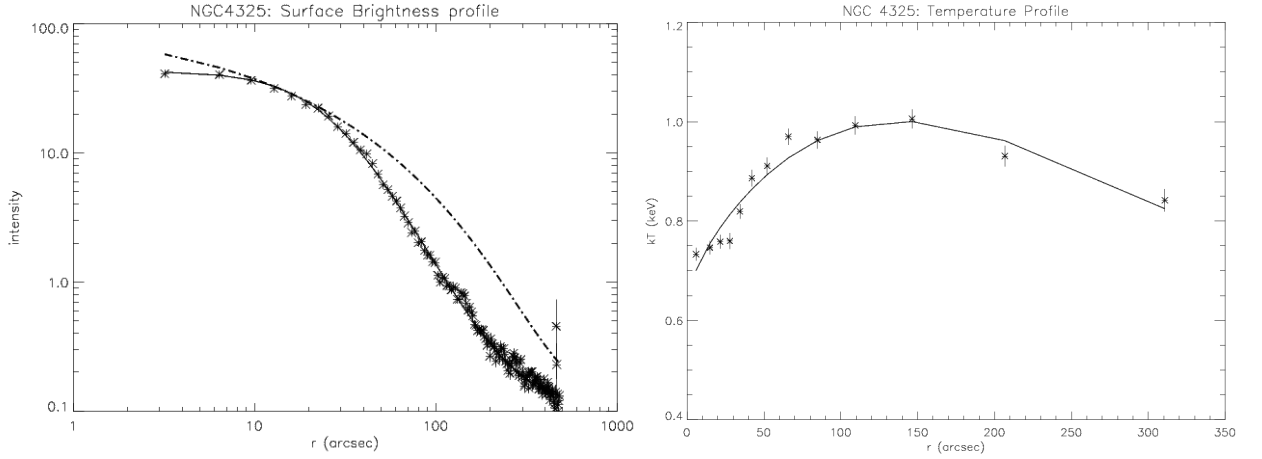
Fig. 2. Left: NGC4325 surface brightness profile. The full curve corresponds to the beta-model while the dashed curve corresponds to the Sersic model. **Right:** NGC4325 temperature profile.

cameras, since they present less bad columns and pixels than the pn camera.

The mean temperature was used to estimate the r_{2500} radius of each group via a kT–r_{2500} scaling relation drawn from Sun et al. (2009). The surface brightness profile is well fitted by a β-model (see left part of Fig. 2):

$$\Sigma(r) = \Sigma_0(1 + (\frac{r}{r_c})^2))^{-3\beta + \frac{1}{2}} \tag{3.1}$$

where r_c is the core radius, β a shape parameter and Σ_0 the central surface brightness. The temperature profile is then fitted by the following expression from Laganá et al. (2008):

$$T_{2D}(r) = \frac{T_0(\alpha\sqrt{\frac{r}{r_t}} + \frac{r}{r_t} + 1)}{(\frac{r}{r_t})^2 + 1} \tag{3.2}$$

where r_t is a scale parameter, T_0 the central temperature and α a shape parameter. Assuming the β-model, one can get the gas density profile from the surface brightness profile.

$$\rho(r) = \rho_0(1 + (\frac{r}{r_c})^2)^{-\frac{3\beta}{2}} \tag{3.3}$$

where r_c and β are the parameters of the β-model fitting the surface brightness profile and ρ_0 is calculated taking into account the normalization parameter in XSPEC. The gas mass in a radius of r_{2500} is simply obtained by integrating the density profile over a sphere of radius r_{2500}.

Assuming the gas is a perfect gas in hydrostatic equilibrium in the Newtonian potential of the group, one can write the following equation for the dynamical mass:

$$M_{dyn}(r) = -\frac{r^2 kT(r)}{m_H G\mu}(\frac{1}{\rho(r)}\frac{d\rho(r)}{dr} + \frac{1}{T(r)}\frac{dT(r)}{dr}) \tag{3.4}$$

where m_H, G, μ and k are respectively the proton mass, the gravitational constant, the average molar mass and the Boltzmann constant. We thus calculate the total mass within r_{2500} using the density and temperature profiles.

4   Discussion

The method described above enables us to calculate the fraction of baryons in stars ($f_{stars} = \frac{M_{stars}}{M_{tot}}$), in gas ($f_{gas} = \frac{M_{gas}}{M_{tot}}$) and the total baryon fraction ($f_{baryons} = f_{stars} + f_{gas}$) within a sphere of radius r_{2500} (see Table 1). The values given in Table 1 are somewhat lower than cluster values found in the literature. However, a comparison is possible by considering the evolution of these fractions with the total mass of groups or clusters, as shown in Fig. 3.
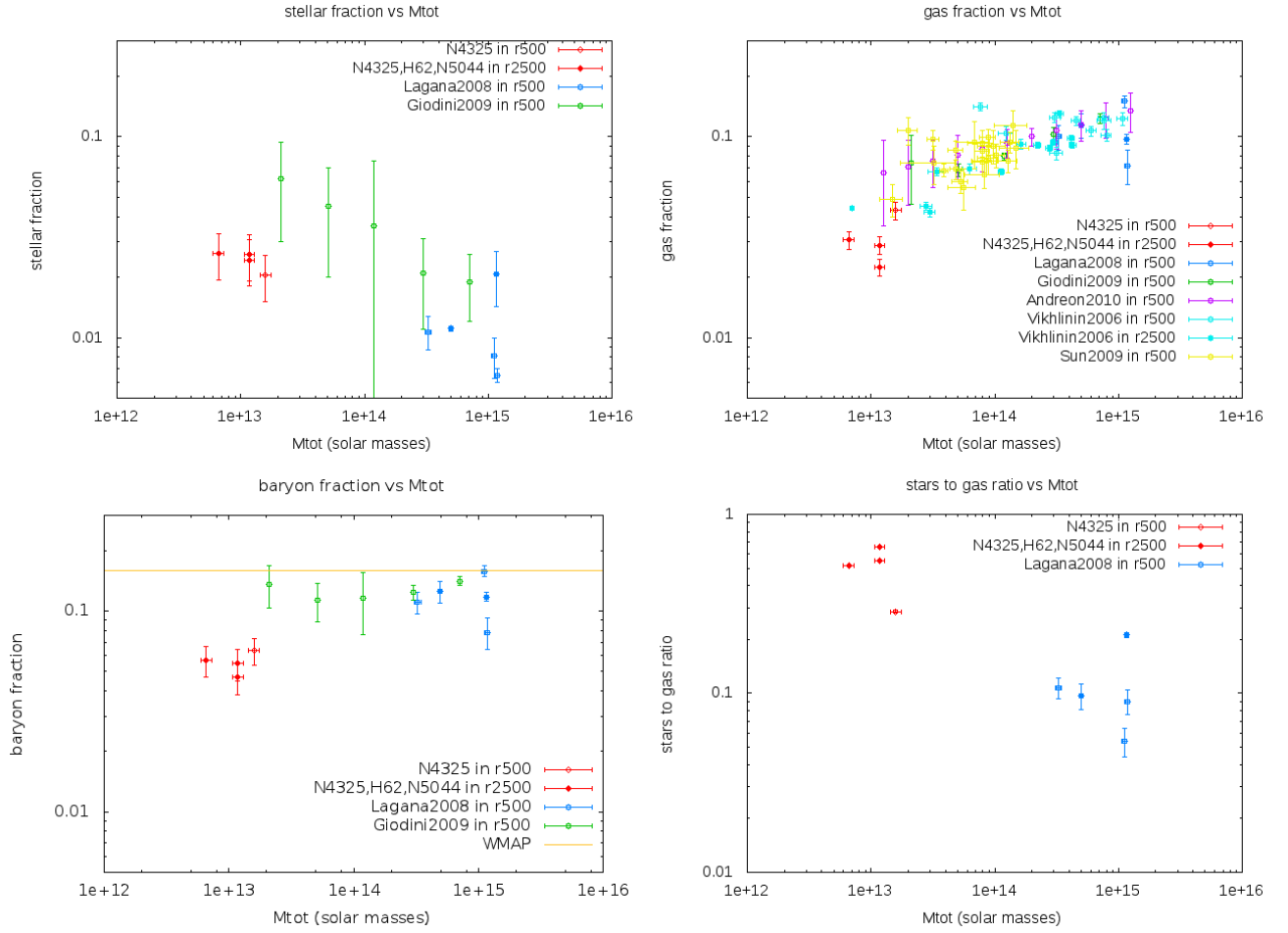
Fig. 3. Top left: Stellar fraction vs total mass. **Top right:** Gas fraction vs total mass. **Bottom left:** Baryon fraction vs total mass. **Bottom right:** stellar to gas mass ratio vs total mass. Open circles are calculated in r_{500} while full circles are in r_{2500} in all figures.

One can notice the different trends of each curve: the stellar fraction decreases with total mass, while the gas fraction increases with total mass. This result lets us think that stars and gas exchange some matter, perhaps by gas accretion or supernova explosions. We plotted values in r_{500} and in r_{2500}. As group studies are only beginning, many results are only given in r_{500}, the usual radius of cluster studies in the literature. We see that our values are in good agreement with values taken from the literature concerning the gas fraction in both r_{500} (Vikhlinin et al. 2006, Sun et al. 2009, Giodini et al. 2009, Andreon 2010) and r_{2500} (Vikhlinin et al. 2006). However, we found lower stellar fractions than those predicted by other studies (Giodini et al. 2009).

This is not surprising for groups calculated within r_{2500} as Giodini et al. worked within a bigger radius: r_{500}, and thus their groups contain much more baryons. However, we calculated NGC4325 values within r_{500} and it still has lower stellar and baryon fractions. The main argument that could account for this result is the contribution of diffuse light, which has been neglected due to the difficulty to detect it. Diffuse light is the part of stellar matter which is not in a galaxy but is located in the intracluster medium. As groups are less dominated by gravitation than clusters, this diffuse light could account for much more missing baryons in groups than in clusters. For example, Da Rocha et al. (2008) showed that this matter could account for almost half of the total stellar mass in some groups. As a result of our lower stellar masses, our baryon fractions are also lower than expected from the literature (Giodini et al. 2009).

Diffuse light could therefore be a major constituent of the baryon fraction and thus partially explain the lack of baryons compared to the WMAP value ($\frac{\Omega_B}{\Omega_M} = 0.16$, Dunkley et al. 2009). Another explanation for this lack of baryons could be that we do measurements in a small radius (r_{2500} or r_{500}) while the WMAP value is

Table 1. Baryon fractions in r_{2500} for a sample of four groups (the quality of the X-ray data for HCG42 was not sufficient to derive the gas and total masses). NGC5846 is not distant enough to be studied in this radius, so it is analyzed in $0.67r_{2500}$). We also give values in r_{500} for NGC4325.

Groups	z	r_{2500}	T_X	M_{tot} ($10^{11}M_\odot$)	f_{stars}	f_{gas}	$f_{baryons}$
NGC4325	0.0257	171	0.84±0.01	118±11.8	0.0243±0.0063	0.0224±0.002	0.0467±0.0083
HCG62	0.0137	168	0.81±0.03	66±6.6	0.0262±0.0068	0.0306±0.0031	0.0568±0.0099
HCG42	0.0133	157	0.69±0.02				
NGC5044	0.0093	175	0.88±0.03	118±11.8	0.0259±0.0067	0.0288±0.0029	0.0547±0.0096
NGC5846	0.0057	155	0.67±0.01	77.5±7.8	0.0107±0.0028	0.0068±0.0007	0.0175±0.0035
Groups	z	r_{500}	T_X	M_{tot} ($10^{11}M_\odot$)	f_{stars}	f_{gas}	$f_{baryons}$
NGC4325	0.0257	364	0.84±0.01	159±15.9	0.0204±0.0053	0.0430±0.0043	0.0634±0.0096

obtained for all the sky.

Finally, we plotted the ratio of the stellar mass to gas mass against the total mass. While comparing our sample with clusters of Laganá et al. (2008), we can conclude that this ratio decreases with total mass. This underlines the importance of calculating accurately the stellar mass in the case of groups. In most cluster studies the stellar mass is simply estimated as one sixth of the gas mass while here it almost reaches one half (and this without taking into account diffuse light).

References

Andreon, S. 2010, MNRAS, 407, 263

Bertin, E 2002, ASP, Vol. 281, p. 228

Bertin, E. 2006, ASP, Vol. 351, p. 112

Bertin, E. & Arnouts, S. 1996, A&AS 317, 393

Da Rocha, C., Ziegler, B.L., Mendes de Oliveira, C. 2008, MNRAS, 388, 1433

Dunkley J. et al. 2009, ApJS, 180, 306

Durret, F., Slezak, E. & Adami, C. 2009, A&A, 506, 637

Giodini, S., et al. 2009, ApJ, 703, 982

Kauffmann, G., et al. 2003, MNRAS, 341, 33

Laganá T. F., Lima Neto G. B., Andrade-Santos, F., and Cypriano E. S. 2008, A&A, 485, 633

Osmond, J. P. F., Ponman, T. J. 2004, MNRAS, 350, 1511

Robin, A. C., Reylé, C., Derrière, S., Picaud, S. 2003, A&A, 409

Schlegel, D.J., Finkbeiner, D. P., Davis, M. 1998, ApJ, 500, 525

Sun, M., et al. 2009, ApJ, 693, 1142

Vikhlinin A., et al. 2006, ApJ, 640, 691